

# Cold- and salinity stress-induced bipolar pea DNA helicase 47 is involved in protein synthesis and stimulated by phosphorylation with protein kinase C

Ajay Amar Vashisht, Arun Pradhan, Renu Tuteja and Narendra Tuteja\*

International Centre for Genetic Engineering and Biotechnology, Aruna Asaf Ali Marg, New Delhi 110 067, India

Received 29 April 2005; revised 20 June 2005; accepted 6 July 2005.

\*For correspondence (fax +91 11 26162316; e-mail narendra@icgeb.res.in).

## Summary

Helicases are involved in the metabolism of nucleic acid; this is very sensitive to the abiotic stresses that reduce plant growth and productivity. However, the molecular targets responsible for this sensitivity have not been well studied. Here we report on the isolation and characterization of cold- and salinity stress-induced pea DNA helicase 47 (PDH47). The transcript of *PDH47* was induced in both shoots and roots under cold (4°C) and salinity (300 mM NaCl) stress, but there was no change in response to drought stress. Tissue-specific differential regulation was observed under heat (37°C) stress. ABA treatment did not alter expression of *PDH47* in shoots but induced its mRNA in roots, indicating a role for PDH47 in both the ABA-independent and ABA-dependent pathways in abiotic stress. The purified recombinant protein (47 kDa) contains ATP-dependent DNA and RNA helicase and DNA-dependent ATPase activities. With the help of photoaffinity labeling, PDH47 was labeled by [ $\alpha$ -<sup>32</sup>P]-ATP. PDH47 is a unique bipolar helicase that contains both 3' to 5' and 5' to 3' directional helicase activities. Anti-PDH47 antibodies immunodeplete the activities of PDH47 and inhibit *in vitro* translation of protein. Furthermore, the PDH47 protein showed upregulation of protein synthesis. The activities of PDH47 are stimulated after phosphorylation by protein kinase C at Ser and Thr residues. Western blot analysis and *in vivo* immunostaining, followed by confocal microscopy, showed PDH47 to be localized in both the nucleus and cytosol. The discovery of cold- and salinity stress-induced DNA helicase should make an important contribution to a better understanding of DNA metabolism and stress signaling in plants. Its bipolar helicase activities may also be involved in distinct cellular processes in stressed conditions.

**Keywords:** abiotic stress, DEAD-box protein, DNA-dependent ATPase, *Pisum sativum*, plant DNA helicase, translation initiation factor, unwinding enzyme.

## Introduction

DNA helicases are motor proteins that catalyze the unwinding of duplex DNA in an ATP-dependent manner and thereby play an important role in most of the basic genetic processes including replication, repair, recombination, transcription and translation (Lohman and Bjornson, 1996; Matson *et al.*, 1994; Tuteja and Tuteja, 2004a,b). Usually they need single-stranded (ss) DNA or a ss/double-stranded (ds) DNA junction as the loading zone and translocate on DNA in either the 3' to 5' or the 5' to 3' direction (Lohman and Bjornson, 1996; Matson *et al.*, 1994). RNA helicases catalyze the ATP-dependent unwinding of local RNA secondary structures and play a broader role in remodeling RNA structures (Gorbalenya *et al.*, 1989; Linder *et al.*, 1989; Luking *et al.*, 1998; Pause and Sonenberg, 1992). Multiple

DNA helicases are present in cells to deal with the different structural requirements of the substrate in the various DNA processes (Lohman and Bjornson, 1996; Matson *et al.*, 1994; Tuteja and Tuteja, 1996). For example, at least 14 different DNA helicases have been reported from *Escherichia coli*, six from bacteriophages, 12 from other viruses, 15 from yeast, 11 from calf thymus and 25 from humans (Tuteja and Tuteja, 2004a). However, the exact biological roles of only a few DNA helicases have been defined (Lohman and Bjornson, 1996; Matson *et al.*, 1994; Tuteja and Tuteja, 2004b). To date very little is known about DNA helicases from plants, of which only six have been reported in purified form (Tuteja, 2003; Tuteja and Tuteja, 2004a). Using cDNA microarray analysis of 1300 Arabidopsis genes, Seki *et al.* (2001)

reported a DEAD-box helicase gene (accession no. AB050574) as a cold stress-inducible gene, suggesting a new role for helicases in stress signaling.

Plants encounter a wide range of environmental insults during their typical life cycle. Their responses to abiotic stresses are multigenic and the molecular mechanisms underlying these responses are not very well understood. Previously, DEAD-box helicase genes were reported to be induced under conditions of chilling and freezing stress (Chamot *et al.*, 1999; Gong *et al.*, 2002). Here we report the cloning and characterization of the cold- and salinity stress-induced pea DNA helicase 47 gene (*PDH47*), which encodes a dual helicase (PDH47). Interestingly it contains bidirectional DNA helicase activity and is shown to be involved in initiation of protein translation. The activities of PDH47 were stimulated by phosphorylation with protein kinase C (PKC). Finally we also show that PDH47 is localized in both the nucleus and the cytoplasm.

## Results

### *Isolation and sequence analysis of pea PDH47 cDNAs*

For cDNA cloning, partial fragments of about 0.8 kb encoding a cold stress-induced helicase were amplified by PCR using cold-stressed ds-cDNA as template and degenerate primers designed from the conserved helicase motifs I and VI. Two cDNA clones (pBS-*PDH47-1* and pBS-*PDH47-2*) were obtained after screening a pea cDNA library with the partial fragment (0.8 kb) as the probe. Sequence analysis of pBS-*PDH47-1* cDNA (accession no. AY167670) shows that it encodes a full-length cDNA, 1.646 kb in size, with an open reading frame (ORF) of 1.239 kb, a 5' untranslated region (UTR) of 0.147 kb and a 3' UTR of 0.260 kb including an 18 bp poly(A) tail. The sequence analysis of pBS-*PDH47-2* cDNA (accession no. AY167671) shows that it also encodes a full-length cDNA which is 1.638 kb in size with an ORF of 1.239 kb, a 5' UTR of 0.082 kb and a 3' UTR of 0.317 kb including a 19 bp poly(A) tail. The two clones were 92% identical. Thereafter, further work was performed with only clone pBS-*PDH47-1*. The deduced amino acid sequence revealed a protein of 413 amino acid residues with a calculated molecular mass of 47 kDa and a pI of 5.39. Amino acid sequence alignment of PDH47 revealed the highest identity (93%) to be with tobacco eIF4A (accession no. X79009). PDH47 exhibits all nine canonical helicase motifs including the newly discovered Q motif.

### *Tissue distribution and regulation of PDH47 transcript levels in response to abiotic stresses*

The transcript levels of *PDH47* in different organs of pea were studied by Northern hybridization. The results showed a single transcript of approximately 1.6 kb in pea shoots and

roots but not in flowers or tendrils after washing the blot at both low stringency (data not shown) and at high stringency (Figure 1a). The transcript was of the expected size for *PDH47* mRNAs. The transcript level was higher in the shoots than in the roots (Figure 1a, lanes 2 and 1, respectively). To analyze *PDH47* expression under various abiotic stresses, 7-day-old pea seedlings were treated with the indicated stresses for different times. Control plants were treated in the same manner with water. Total RNAs were extracted from control and treated shoot and root tissues and hybridized with the ORF of *PDH47* cDNA probes. The results are shown in Figure 1 (panels b, d, f, h, j for shoots and c, e, g, i, k for roots). The quantitative data are also shown as histograms on top of the autoradiograms. The upregulation of *PDH47* transcripts was observed in both shoots and roots of the cold (panels b and c) and salinity (panels d and e) stress-treated pea plants. Following treatment at low temperature (4°C), the transcript increased after 6 h, reaching a maximum at 24 h both in shoots and roots (Figure 1b,c). After NaCl (300 mM treatment, the level increased after 6 h both in shoot and root (Figure 1d,e). Interestingly, in response to drought stress the transcript level of the *PDH47* gene did not alter in either shoots (Figure 1f) or roots (Figure 1g). In response to heat (37°C) stress, an opposite effect was observed in shoots (downregulation) and roots (upregulation) (Figure 1h,i, respectively). Finally, after treatment with abscisic acid (ABA), the level of transcript did not change in shoots (Figure 1j) but increased in roots (Figure 1k).

### *Expression, purification and characterization of PDH47 protein*

The pea cDNA encoding PDH47 was cloned into a bacterial expression vector pET28a (pET28a-*PDH47*) and the recombinant His-tagged protein was expressed in *E. coli*. The recombinant PDH47 was present in the soluble fraction and purified by Ni<sup>2+</sup>/NTA-agarose and heparin Sepharose column chromatography. Sodium dodecyl sulfate polyacrylamide gel electrophoresis (SDS-PAGE) analysis showed a 47 kDa polypeptide induced by isopropyl β-D-thiogalactopyranoside (IPTG) in *E. coli* transformed with pET28a-*PDH47* (Figure 2a, lane 2) (compare with the uninduced run in lane 1). A single Ni<sup>2+</sup>/NTA agarose column chromatography step yielded almost 95% pure PDH47 protein (Figure 2a, lane 3). The PDH47 was further purified to homogeneity by passing through heparin Sepharose (Figure 2a, lane 4). An antibody raised against the PDH47 protein detects it as a single band of 47 kDa in IPTG-induced, Ni<sup>2+</sup>/NTA agarose and heparin Sepharose fractions (data not shown). These purification protocols routinely yielded about 10 mg of homogeneous PDH47 from 1 l of bacterial culture.

The DNA-unwinding activity of PDH47 was characterized by assaying the displacement of <sup>32</sup>P-labeled DNA from a partial duplex DNA substrate. The substrate used for most of

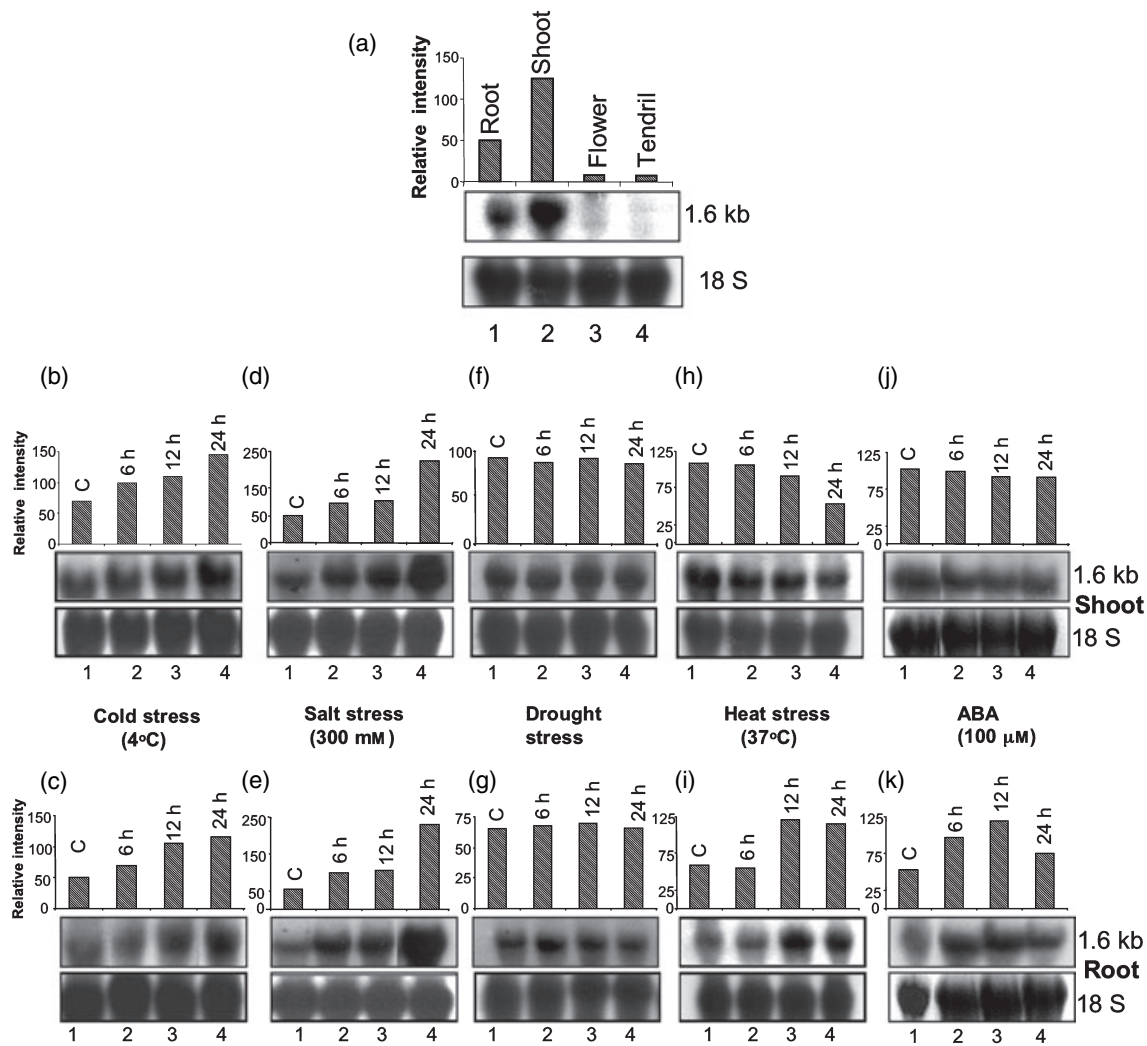


**Figure 1.** Analysis of PDH47 transcripts in response to abiotic stresses in pea shoots and roots.

(a) Northern blot analysis. Total RNA (30  $\mu$ g) was separated by electrophoresis, blotted and hybridized with the  $^{32}$ P-labeled ORF of *PDH47* cDNA (1.239 kb). For equal loading of RNA in each lane, the same blot was hybridized with the *18S* rRNA gene, as shown in the bottom panel. Lanes 1 to 4 contain RNAs isolated from root, shoot, flower and tendrils tissue, respectively.

(b–k) Transcript level in shoot and root tissue in response to stress. The total RNAs were extracted from shoot and root tissue after stress treatment. The various abiotic stresses used were cold (b and c), salinity (d and e), drought (f and g), heat (h and i) and ABA (j and k). The RNA (30  $\mu$ g) samples were separated by electrophoresis, blotted and hybridized with the  $^{32}$ P-labeled ORF of *PDH47* cDNA. For each stress examined in shoots (b, d, f, h, j) and roots (c, e, g, i, k) the upper panel shows the quantitative data, the middle panel shows the autoradiograph of *PDH47* transcript (1.6 kb) and the lower panel shows the hybridization of the same blot with the *18S* rRNA gene (loading control). In each panel lane 1 is the control without any treatment while lanes 2, 3 and 4 are the RNA samples collected after 6, 12 and 24 h of stress treatment.

the characterization contains hanging tails of 15 bp on both the 5' and 3' ends, as shown in Figure 2b. DNA-unwinding activity was measured by using approximately 1 ng of substrate (40  $\mu$ M or 0.40 fmol/10  $\mu$ l) with 10 ng of PDH47 enzyme (20 nM or 0.20 pmol/10  $\mu$ l). The purified enzyme shows DNA-unwinding activity (Figure 2b–g). The enzyme loses the activity upon heating at 56°C for 3 min or after prolonged storage at 4°C (data not shown). The DNA helicase activity is destroyed by trypsin and is inhibited by EDTA (5 mM), sodium phosphate (100 mM), NaCl (200 mM) or 45 mM ammonium sulfate (data not shown). The activity is only around 50% inhibited by M13 ssDNA (30  $\mu$ M as phos-

phate), while M13 dsDNA and yeast tRNA (30  $\mu$ M as phosphate) had almost no effect (data not shown). Interestingly, the enzyme shows good activity over a broad pH range from 5 to 10 (Figure 2b, lanes 3–10) with an optimum activity at pH 8 and 9 (lanes 8 and 9, respectively). There is no activity in the absence of ATP (Figure 2c, lane 2). The ATP concentration curve (Figure 2c) shows its maximum at 2 mM (lane 6), while the activity is inhibited over 8 mM (lane 10). ATP and dATP are the best-utilized cofactors (Figure 2d, lanes 2 and 3) while other nucleotide triphosphates (NTPs)/deoxyNTPs (dNTPs) such as guanosine triphosphate (GTP), dGTP, cytidine triphosphate (CTP), dCTP, thymidine triphosphate (TTP)

and uridine triphosphate (UTP) did not support the activity (Figure 2d, lanes 4–9). There is no activity if ATP is replaced by ADP or AMP or the poorly hydrolysable ATP analog ATP $\gamma$ S (data not shown). The enzyme is also Mg $^{2+}$  dependent, as it did not show activity in the absence of Mg $^{2+}$  (Figure 2e, lane 2). The Mg $^{2+}$  concentration curve (Figure 2e, lanes 3–9) shows optimum activity at 0.5 mM (lane 5), while the activity is reduced at 5 mM Mg $^{2+}$  (lane 9). It shows equally good activity whether the source of Mg $^{2+}$  is MgCl $_2$  or MgSO $_4$

(Figure 2f, lanes 2 and 3). In the presence of Mn $^{2+}$  the enzyme shows similar activity (Figure 2f, lane 4) to that with Mg $^{2+}$ . However, with Ca $^{2+}$  and Zn $^{2+}$  very little activity was seen (lanes 5 and 8). Other divalent cations, such as Ni $^{2+}$ , Cu $^{2+}$ , Co $^{2+}$  and Ag $^{2+}$ , were unable to support the activity (Figure 2f, lanes 6, 7, 10 and 11). The overall divalent cation requirement was Mg $^{2+}$  = Mn $^{2+}$  > Zn $^{2+}$  > Ca $^{2+}$ . The enzyme shows optimum activity at 75 mM KCl (Figure 2g, lane 3), while above 200 mM KCl the enzyme activity is inhibited (lanes 7, 9 and 10). The enzyme did not show ATPase activity in the absence of ssDNA and Mg $^{2+}$  (data not shown). The ssDNA-dependent ATPase activity was present at a level of about 2.0 nmol ATP hydrolyzed in 60 min by 10 ng of pure PDH47 protein.

The ATP-binding activity of PDH47 is shown in Figure 2(h) (Coomassie stained gel) and Figure 2(i) (autoradiogram of the same gel). For affinity labeling, the protein was incubated with [ $\alpha$ - $^{32}$ P]-ATP on ice in the presence of UV light followed by SDS-PAGE (Figure 2h) and autoradiography of the gel (Figure 2i). The results showed that both the 47 kDa polypeptide of PDH47 and the 100 kDa *E. coli* DNA polymerase I as positive control (Figure 2h, lanes 2 and 3) bind radioactive ATP and showed the respective radioactive bands in the autoradiogram (Figure 2i, lanes 2 and 3)

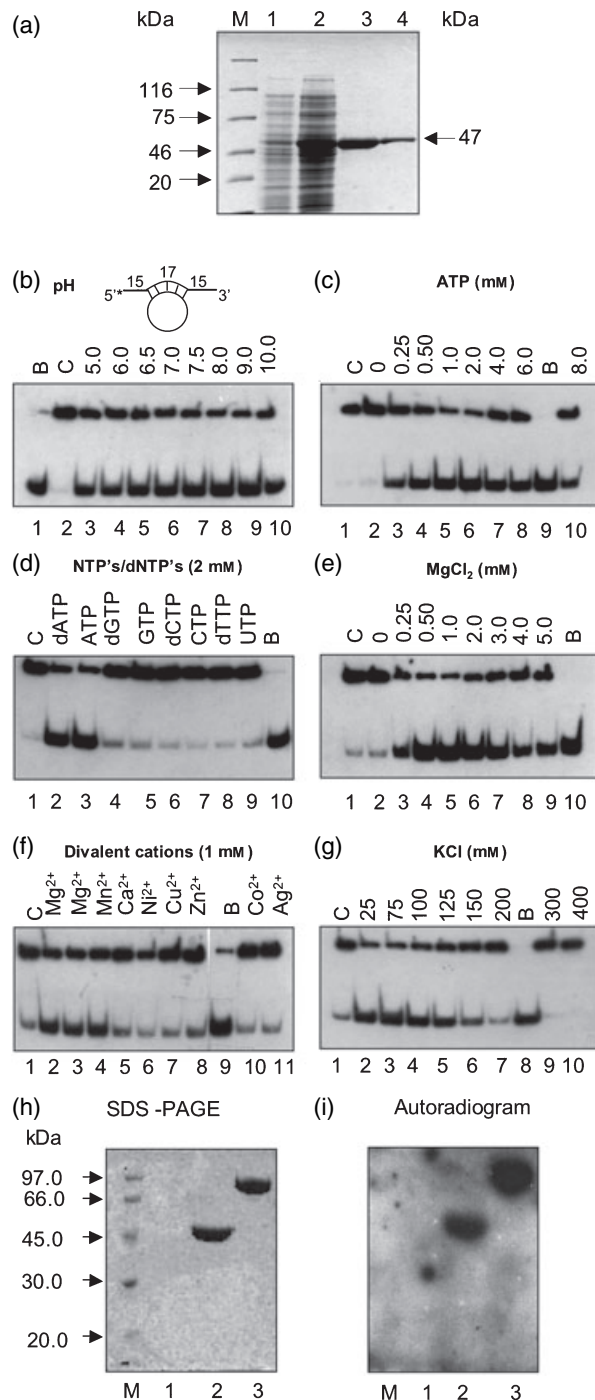


**Figure 2.** Purification of recombinant PDH47 protein from bacteria and its DNA-unwinding and ATP-binding activities.

(a) Induction and purification of PDH47 from *E. coli* is shown on SDS-PAGE. Lane M is a molecular weight marker. Lane 1 is uninduced, lane 2 is IPTG-induced, lane 3 is PDH47 protein after Ni $^{2+}$ /NTA-agarose column and lane 4 is purified PDH47 after heparin Sepharose column chromatography. The protein size markers are indicated to the left side of the gel.

(b–g) DNA-unwinding activity of purified PDH47. The DNA helicase substrate used in panels (b) to (g) contains 15 bp hanging tails at both the 3' and 5' ends as shown in the upper half of panel (b). Asterisks on the substrate denote the  $^{32}$ P-labeled end. The standard helicase reaction was performed by using 10 ng of pure PDH47 protein (20 nM or 0.20 pmol/10  $\mu$ l) with about 1 ng of  $^{32}$ P-labeled helicase substrate (40 pM or 0.40 fmol/10  $\mu$ l). In each autoradiogram, lanes C (control) and B (boiled) show the reaction without enzyme and reaction with heat-denatured substrate, respectively.

(b) pH dependence of DNA unwinding by PDH47. The standard helicase reactions were performed under acidic and basic pH conditions. In lanes 3 to 10, the different pH buffers used were pH 5, 6, 6.5, 7, 7.5, 8, 9 and 10, respectively.

(c) ATP-dependent reaction. The standard helicase reactions were performed with varying concentrations of ATP, mentioned on top of each lane of the autoradiogram.

(d) Preference of nucleotides triphosphate for PDH47 activity. The standard helicase reactions were performed in the presence of one of the NTPs or dNTPs (2 mM). The different NTPs or dNTPs used are mentioned on the top of each lane.

(e) Effect of MgCl $_2$  on the DNA-unwinding activity of PDH47. The standard helicase reactions were carried out in varying concentrations of MgCl $_2$ , shown above each lane of the autoradiogram.

(f) Preference of divalent cations for DNA-unwinding activity of PDH47. The helicase reactions were performed in the presence of either 0.5 mM Mg $^{2+}$  (lanes 2 and 3) or different divalent cations (0.5 mM): Mn $^{2+}$ , Ca $^{2+}$ , Ni $^{2+}$ , Cu $^{2+}$ , Zn $^{2+}$ , Co $^{2+}$ , or Ag $^{2+}$  (lanes 4 to 8, 9 and 10, respectively).

(g) Effect of KCl on the DNA-unwinding activity of PDH47. The standard helicase reactions were carried out in varying concentrations of KCl, shown above each lane of the autoradiogram.

(h, i) Ultraviolet cross-linking of ATP. (h) Coomassie-stained SDS-PAGE gel after the UV cross-linking reaction. Lane M contains protein molecular weight markers. Lane 1, [ $\alpha$ - $^{32}$ P]-ATP was incubated without any protein. (i) Autoradiogram of photoaffinity-labeled *E. coli* DNA polymerase I as a positive control (lane 3) and PDH47 protein (lane 2) with [ $\alpha$ - $^{32}$ P]-ATP. All these data were reproducible and the experiments were repeated at least three times.

indicating that ATP does bind to the PDH47 protein. The labeling reaction was also performed in the absence of the protein (Figure 2h,i, lane 1) in order to observe the background. Competition with increasing concentrations of unlabeled ATP showed the appropriate reduction in intensity of the radioactive band (data not shown).

#### Bidirectional DNA-unwinding activity of PDH47

To determine the direction of translocation of PDH47, four substrates, two specific for the 3' to 5' direction (Figure 3a,c, top panel) and another two for the 5' to 3' direction (Figure 3b,d, top panel), were constructed. DNA-unwinding activity was carried out using approximately 1 ng of different direction-specific substrates (40  $\mu\text{M}$  or 0.40 fmol/10  $\mu\text{l}$ ) and 5 and 10 ng of PDH47 enzyme (10 nM or 0.10 pmol/10  $\mu\text{l}$ , and 20 nM or 0.20 pmol/10  $\mu\text{l}$ ) as shown in Figure 3(a–d) (bottom panels). The release of radiolabeled DNA from the substrates of Figure 3(a,c) and from the substrates of Figure 3(b,d) by PDH47 enzyme indicate movement in the 3' to 5' and 5' to 3' directions, respectively. The results showed that PDH47 could unwind all four substrates (Figure 3a–d), indicating its bidirectional DNA-unwinding activity. However, it showed a little more DNA-unwinding activity with the 3' to 5' direction-specific substrates (Figure 3a,c) than with the 5' to 3' direction-specific substrates (Figure 3b,d). The direction-specific activities of PDH47 were also dependent on ATP/Mg<sup>2+</sup>, as shown by kinetic measurements and catalytic concentrations of the protein (data not shown).

#### Immunodepletion of DNA-unwinding and ATPase activities of PDH47 by antibodies

Purified recombinant His-tagged PDH47 protein was individually reacted with immunoglobulin G (IgG) purified from pre-immune rabbit serum and antiserum raised against PDH47 protein, as well as with anti-His monoclonal antibody. Protein A Sepharose beads were used to remove the antigen–antibody complex. The supernatant was analyzed for DNA helicase and ATPase activities under standard assay conditions using hanging tail substrates (as shown on the left-hand side of Figure 4a) for helicase and radioactive [ $\gamma$ -<sup>32</sup>P]-ATP for ATPase. Activities of both the DNA helicase (Figure 4a, lanes 3 and 4) and the ATPase (Figure 4b, lanes 3 and 4) were depleted by anti-PDH47 IgG and anti-His antibodies, respectively. There was no reduction in activity using the pre-immune IgG (Figure 4a,b, lane 2).

#### DNA–RNA and RNA helicase activity of PDH47

PDH47 shows Mg<sup>2+</sup>- and ATP-dependent DNA–RNA helicase activity (Figure 4c, lane 4). It fails to unwind the substrate in the absence of Mg<sup>2+</sup> and ATP (Figure 4c, lanes 2 and 3, respectively). In addition, PDH47 protein also has RNA-

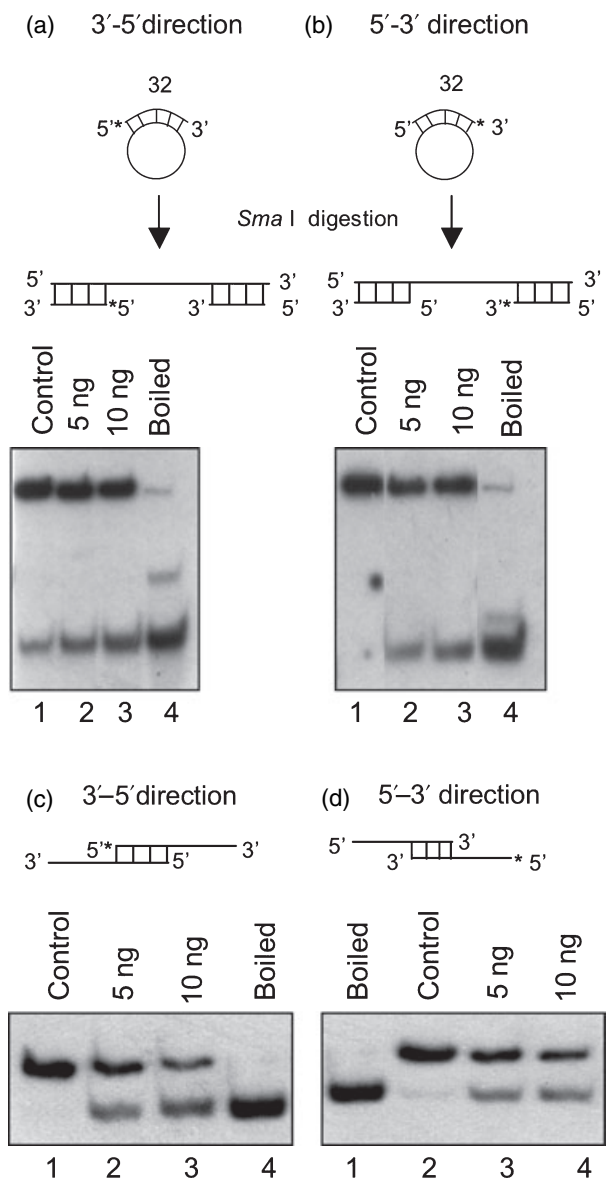


**Figure 3.** Bipolar DNA-unwinding activity of PDH47.

The construction and structure of the linear substrates for the 3' to 5' direction (a and c) and the 5' to 3' direction (b and d) are shown on top of the autoradiogram. In each gel, lane 1 is the reaction without enzyme (control) and lanes 2 and 3 are the reaction with 5 and 10 ng of pure PDH47 protein, respectively. Lane 4 is the boiled substrate. The asterisk denotes the <sup>32</sup>P-labeled end. These experiments were repeated at least three times.

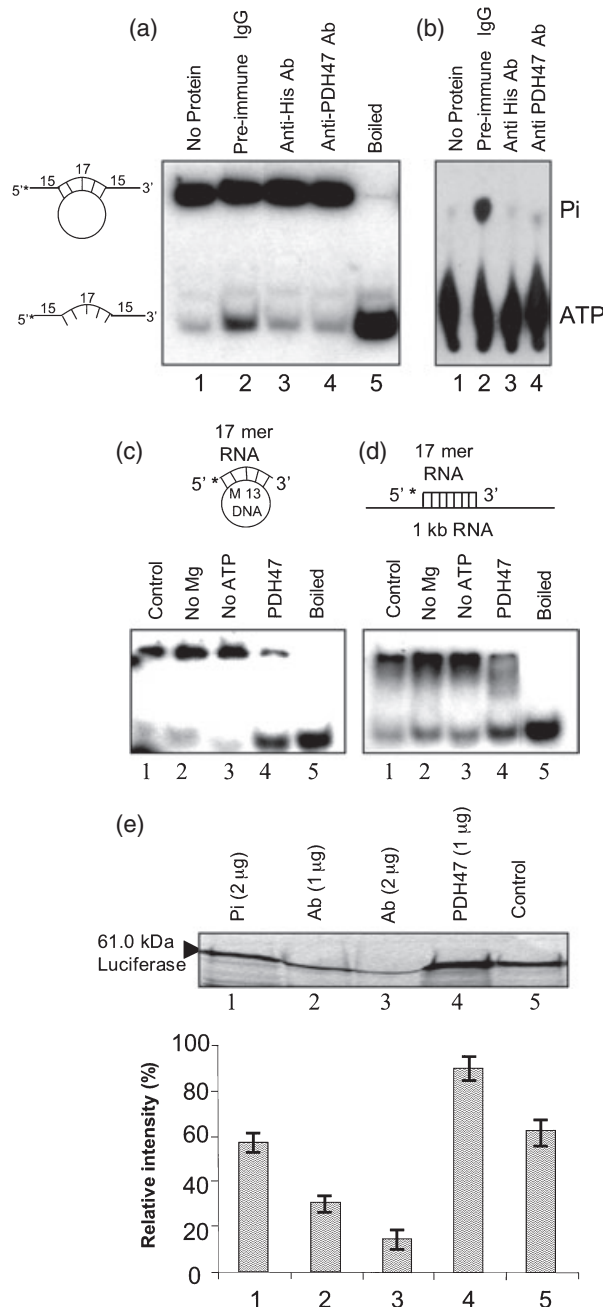
unwinding activity (Figure 4d, lane 4). This RNA unwinding was also Mg<sup>2+</sup> and ATP dependent (Figure 4d, lanes 2 and 3, respectively). The RNA helicase activity was also immunodepleted in a specific manner (data not shown).

#### Function of PDH47 in translation of proteins

To study the effect of PDH47 on translation of protein, anti-PDH47 antibody was used in an *in vitro* transcription–

translation coupled assay performed with firefly luciferase mRNA using a wheat germ lysate system (Promega, Madison, WI, USA). Since PDH47 contains about 91% identity at the amino acid level with wheat germ eIF4A [accession no. Z21510 (gi397632)], the anti-PDH47 antibodies should react with wheat germ eIF4A. *In vitro* translation in the presence of pre-immune rabbit serum IgG (as a control) yielded a 61 kDa luciferase protein (Figure 4e, lane 1). There was no effect of pre-immune IgG on the translational activity of the lysate, as the 61 kDa luciferase protein band showed the same intensity as an untreated lysate (Figure 4e, lane 5). The presence

of 1 µg of purified anti-PDH47 antibodies (IgG) during *in vitro* translation resulted in the inhibition of the translation (Figure 4e, lane 2). Upon further increase in the quantity of antibodies in the reaction to 2 µg, more inhibition of translation was observed (Figure 4e, lane 3). Furthermore, the addition of the purified PDH47 protein (1 µg) to the standard *in vitro* translation reaction resulted in an enhancement of the product (61 kDa luciferase protein) (Figure 4e, lane 4). The intensity of the product band was quantified and the data are shown as a histogram under the autoradiogram (Figure 4e, lower panel).



*In vitro phosphorylation of PDH47 by protein kinase C*

*In vitro* phosphorylation is based on incubating the PDH47 protein with [ $\gamma$ - $^{32}$ P]-ATP in the presence of PKC (from an animal source). Here we have used myelin basic protein (MBP) as a positive control and bovine serum albumin (BSA) as a negative control for the PKC. After incubation, phosphorylation of the proteins was examined by SDS-PAGE followed by autoradiography. The results show that the 47 kDa polypeptide of PDH47 (Figure 5a, lanes 1 and 2) and the 23.3 kDa polypeptide of MBP (Figure 5a, lane 3) were phosphorylated by PKC, while the negative control (66 kDa BSA) did not show any phosphorylation (Figure 5a, lane 4). This phosphorylation was dose dependent, as the extent of phosphorylation increased with increase in the concentration of PDH47 (40 ng, lane 1, 60 ng, lane 2).

**Figure 4.** Immunodepletion of DNA helicase and ATPase activities and DNA-RNA- and RNA-unwinding activities of PDH47 and its function in *in vitro* translation.

(a) Immunodepletion of DNA helicase activity. Lane 1, control without enzyme. Lane 2, PDH47 treated with pre-immune IgG. Lane 3, PDH47 treated with anti-His monoclonal antibody. Lane 4, PDH47 treated with anti-PDH47 IgG. Lane 5, heat-denatured substrate. The structure of the hanging-tail substrate used for the assay is shown to the left-hand side of the gel. (b) Immunodepletion of ATPase activity. Lane 1, control without enzyme. Lane 2, PDH47 treated with pre-immune IgG. Lane 3, PDH47 treated with anti-His monoclonal antibody. Lane 4, PDH47 treated with anti-PDH47 IgG. The positions of the inorganic phosphate (Pi) and ATP are marked on the right-hand side of the thin layer chromatogram. (c, d) DNA-RNA- and RNA-unwinding activities of PDH47. Models of the DNA-RNA and RNA duplex substrates used to detect RNA helicase activity are shown at the top of the respective autoradiograms. The asterisk denotes the  $^{32}$ P-labeled end. In both panels (c) and (d) lane 1 is the reaction without enzyme, lane 2 is the reaction with PDH47 but without  $Mg^{2+}$ , lane 3 is the reaction with PDH47 but without ATP, lane 4 is the reaction with PDH47 protein (10 ng) and lane 5 is the boiled substrate. (e) Inhibition and stimulation of *in vitro* translation with anti-PDH47 antibodies and PDH47 protein, respectively. An *in vitro* translation reaction was performed using a wheat germ lysate system and luciferase mRNA. The 61 kDa luciferase product is shown by an arrow on the left-hand side of the autoradiogram. Lane 1 is a standard reaction in the presence of rabbit pre-immune IgG (2 µg) showing the prominent 61 kDa band. Lanes 2 and 3 are the *in vitro* translation reaction in the presence of two different concentrations (1 and 2 µg) of anti-PDH47 IgG. Lane 4 is the standard *in vitro* translation reaction with additional PDH47 protein. Lane 5 is the control translation reaction without the antibodies and PDH47 protein. The quantitative data are shown as a histogram under the autoradiogram of the gel.

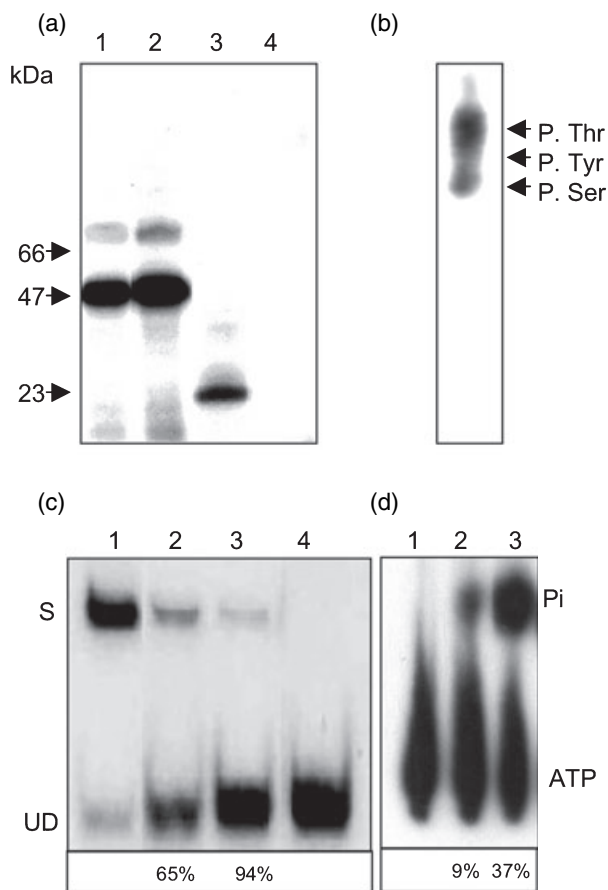


**Figure 5.** *In vitro* phosphorylation and stimulation of DNA helicase and ATPase activities of PDH47 by PKC.

(a) The standard kinase reaction was carried out with  $Mg^{2+}$  and  $[\gamma\text{-}^{32}\text{P}]\text{-ATP}$  followed by SDS-PAGE and autoradiography as described in Experimental procedures. The autoradiogram shows the 47 kDa band of PDH47 phosphorylated with PKC (lanes 1 and 2). The phosphorylation reactions were performed with 40 ng (lane 1) and 60 ng (lane 2) of PDH47 protein. Lane 3 is the reaction with myelin basic protein (MBP) (as a positive control) and lane 4 is BSA (as a negative control).

(b) PDH47 is phosphorylated at Ser and Thr residues. The  $^{32}\text{P}$ -labeled 47 kDa protein was hydrolyzed in 6 N HCl and analyzed by paper chromatography as described in Experimental procedures. The positions of the standard phospho-amino acids visualized by ninhydrin staining are indicated on the right.

(c) DNA helicase activity of PDH47 after phosphorylation with PKC. Lane 1, control without PDH47. Lane 2, PDH47 (10 ng) without PKC (-PKC sample). Lane 3, phosphorylated PDH47 (10 ng) (+PKC sample). Lane 4, heat-denatured substrate. The percentage of unwinding in lanes 2 and 3 is shown at the bottom of the gel. The structure of the hanging tail substrate used is shown in Figure 4(a) (S, substrate; UD, unwound DNA.)

(d) ssDNA-dependent ATPase activity of PDH47 after phosphorylation with PKC. Lane 1, PDH47 (10 ng) without PKC (-PKC sample). Lane 2, PDH47 (10 ng) with PKC (+PKC sample). The percentage of inorganic phosphate (Pi) released in lanes 1 and 2 is shown at the bottom of the autoradiogram. The positions of Pi and ATP are marked on the right-hand side.

#### *PDH47 is phosphorylated at Ser and Thr residues*

The phosphorylated 47 kDa band of PDH47 was eluted from the gel and subjected to phospho-amino acid analysis followed by paper chromatography. This analysis revealed that

phosphorylation occurred on Ser and Thr residues of PDH47 (Figure 5b).

#### *Stimulation of DNA helicase and ATPase activities of PDH47 by phosphorylation*

The effect of PKC phosphorylation on the DNA helicase and ssDNA-dependent ATPase activities of PDH47 was studied. Both the DNA helicase (Figure 5c, lane 3) and ATPase (Figure 5d, lane 3) activities of PDH47 were stimulated after PKC phosphorylation (Figure 5c, lane 2 and Figure 5d, lane 2, respectively). Lane 1 in Figure 5(c,d) is a control reaction without PDH47.

#### *Localization of PDH47 by Western blotting and by immunofluorescence labeling/confocal microscopy*

The result of localization of PDH47 by Western blotting is shown in Figure 6(a). The anti-PDH47 antiserum detected a protein band of about 47 kDa in the cytosol and in the nuclear extract (Figure 6a, lanes 1 and 2) but not in the chloroplast lysate (Figure 6a, lane 3). The purified recombinant PDH47 protein (Figure 6a, lane 4) was used as a control, and this was recognized by the antiserum. The pre-immune serum did not recognize any protein in the same preparation (data not shown). These results also showed that PDH47 is more abundant in the cytosol than the nucleus (Figure 6a). The *in vivo* localization of PDH47 was also analyzed by immunofluorescence labeling followed by confocal microscopy. Immunofluorescent labeling of tobacco BY2 cells with anti-PDH47 antibodies showed the localization of the PDH47 protein in the nucleus and cytosol of all the cells (Figure 6b–d). These results are similar to the localization determined by Western blotting (Figure 6a).

#### **Discussion**

As abiotic stress affects the cellular gene-expression machinery, it is evident that the molecules involved in nucleic acid processing, including helicases, are likely to be affected by stress as well. However, the regulation of biochemically active DNA helicases in response to stress has not been studied. Stress-induced DNA helicases may be essential for survival during times of stress. We have isolated a novel DNA helicase gene (*PDH47*) which is specifically upregulated in response to cold and salinity. Biochemical analysis with purified recombinant PDH47 protein confirmed that it functions as a dual bipolar helicase and ATPase with activity that is enhanced by phosphorylation and having involvement in protein synthesis. It is differentially expressed in different organs (more in shoots compared with roots) and it is not expressed in detectable amount in the flowers or tendrils of pea plants.

In order to understand plant development and the stress response, it is imperative to know the function of essential

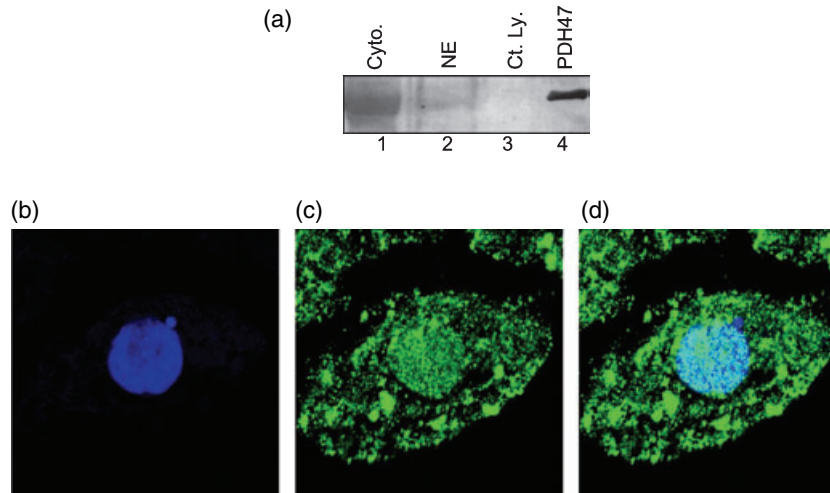


**Figure 6.** Localization of PDH47 in pea by Western blotting and in tobacco BY2 cells by immunofluorescence staining and confocal microscopy. (a) Localization of PDH47 by Western blotting. The cytosol (Cyto., lane 1), nuclear extract (NE, lane 2) and chloroplast lysate (Ct. Ly., lane 3) were prepared from the leaves of pea seedlings and fractionated by SDS-PAGE. Lane 4 is purified PDH47 (after heparin Sepharose column chromatography) as a positive control for the antibody. Proteins were transferred onto a nitrocellulose membrane and Western blots used polyclonal anti-PDH47 antiserum. (b–d) *In vivo* localization. The tobacco BY2 cells were fixed, permeabilized and immunostained with primary antibodies against PDH47 followed by Alexafluor 488-labeled secondary antibody and then counterstained with DAPI. A single confocal image is shown. (b) Image of cell stained with DAPI (blue). (c) Immunofluorescently stained cell (green). Anti-PDH47 labeling is restricted to the nucleus and cytosol. (d) Superimposed image of cell.

genes and their regulation during different phases of the plant life cycle. Cold, drought and salinity are common stress conditions that can adversely affect plant growth and yield. By using a full-length cDNA microarray method, a large number of genes (including one of the DEAD-box helicases, *DRH1*) in Arabidopsis were induced in response to various abiotic stresses (Seki *et al.*, 2001) but their functions have not yet been defined. In this study, the transcript level of *PDH47* showed a differential steady-state in response to various abiotic stresses. In general, shoots had a higher level of expression than roots; however, in both tissues there was an upregulation of transcription in response to cold and salinity. A mutant, *los4-1*, which was previously reported to be altered in cold-responsive gene regulation and chilling tolerance, was found to encode a DEAD-box helicase protein (Gong *et al.*, 2002). This also indicated that helicases might be involved in stress signaling. Studies of animal and microbial systems have also suggested a possible upregulation of DEAD-box helicases in response to environmental stresses (Briolat and Reysset, 2002; Liu *et al.*, 2002; Yu and Owttrim, 2000). In barley, the putative RNA helicase gene *HVD1* was induced under salinity stress in shoots (Nakamura *et al.*, 2004). Interestingly, in the present study no significant change in *PDH47* mRNA level was observed in response to drought stress. In response to heat stress, the *PDH47* mRNA was upregulated in root tissue but downregulated in shoot tissue. This tissue-specific dual regulation of *PDH47* by heat stress in roots and shoots could be a novel behavior of this gene. In shoot tissue it was found that *PDH47* mRNA was upregulated at a low temperature (4°C) but downregulated at a higher temperature (37°C). The cold-shock-specific

expression of *PDH47* mRNA is similar to that of the *E. coli* RNA helicase gene *CsdA* (Charollais *et al.*, 2004) and DEAD-box proteins from cyanobacteria (Yu and Owttrim, 2000). However, *PDH47* is not a homolog of these genes. Interestingly, induction of the transcript in roots was mediated by the phytohormone ABA, while in shoots it follows an ABA-independent pathway. This observation will be useful in understanding tissue-specific components involved in ABA signaling in plants. Recently, over-expression of PDH45 has been shown to confer high salinity tolerance without affecting yield, which indicates a role for helicases in stress tolerance (Sanan-Mishra *et al.*, 2005).

PDH47 is active over a broad pH range (pH 5–10). Activity of DNA helicases at acidic pH is not very common, which indicates that this is a novel enzyme functioning specifically during conditions of stress. It uses only ATP or dATP as a cofactor while the previously reported enzyme PDH45 could utilize all the other NTPs/dNTPs as well (Pham *et al.*, 2000). Very interestingly, our studies showed that PDH47 translocates in both the 3' to 5' and 5' to 3' directions along the bound strand. Bipolar helicase activities are not very common among the DEAD-box family of helicases. Recently, bipolar DNA helicase activities have been reported for the PcrA helicase from *Bacillus anthracis* and *Staphylococcus aureus* (Anand and Khan, 2004) and the HerA DNA helicase from thermophilic Archaea (Constantinesco *et al.*, 2004). Anti-PDH47 antibodies (IgG) and anti-His antibodies were shown to immunodeplete the DNA-unwinding and ATPase activities of PDH47 in solution. This study confirms that all the activities are due to the PDH47 polypeptide and not to contamination by any *E. coli* helicases in the preparation. We



observed that PDH47 also contained ATP-dependent RNA as well as DNA–RNA-unwinding activities. The RNA-dependent ATPase activity of PDH47 helps to explain its RNA helicase activity. This study confirms that PDH47 is a dual helicase containing both DNA and RNA helicase activities; there are only a few proteins endowed with both DNA and RNA helicase activity (Tuteja and Tuteja, 2004a).

Regarding the role of PDH47 in translation, we observed that the antibodies against PDH47 inhibit *in vitro* protein synthesis. Furthermore, we also observed that the purified PDH47 protein enhances *in vitro* protein synthesis. These studies confirm the role of PDH47 in protein synthesis. Protein synthesis is very sensitive to stress, so the factors involved in translation could be potentially affected by stress in plants. PDH47 may act at the translational level to enhance or stabilize protein synthesis during conditions of stress in plants. During stress, secondary structures could be created in the 5' UTR of the mRNA of essential proteins which need to be resolved. Since PDH47 is induced during times of plant stress, its RNA helicase activity probably helps to unwind inhibitory structures in the 5' UTR of mRNA, which facilitates binding of the 40S ribosomal subunit and thereby promotes protein synthesis. The mechanisms of translation initiation are conserved among eukaryotes, and the regulation of translation occurs at the step of initiation (Gingras *et al.*, 1999).

This study shows that PDH47 is a substrate of PKC and the activities of PDH47 were stimulated after phosphorylation. Protein kinase C is a Ser/Thr kinase and is known to be involved in gene expression, signal transduction and regulation of the activities of many proteins (Buelt *et al.*, 1994; Tuteja *et al.*, 2003; Yang *et al.*, 2004). This result clearly suggests that phosphorylation plays a role in regulating the enzymatic activities of PDH47. Protein kinase C-dependent phosphorylation also suggests that PDH47 may be involved in signal transduction pathways regulating the cellular functions of the DNA helicase and ATPase activities of the protein. Amino acid analysis showed that both Ser and Thr residues were phosphorylated with PKC. Computer analysis (NetPhos, ExPASy) of amino acid sequences of PDH47 revealed that it contained few potential Ser and Thr sites for PKC phosphorylation. The phosphorylation of tobacco eIF4A8, a pollen-specific isoform, was shown to occur at a Thr residue with an unknown kinase (op den Camp and Kuhlemeier, 1998). Previously, the helicase activity of PDH65 was reported to be upregulated by cdc2 and CK2 phosphorylation (Tuteja *et al.*, 2001). Pea topoisomerase I activity has also been reported to be enhanced by PKC phosphorylation (Tuteja *et al.*, 2003). In contrast, the RNA helicase and ATPase activities of p68 protein are inhibited by PKC phosphorylation (Buelt *et al.*, 1994; Yang *et al.*, 2004). Overall, the results of phosphorylation studies suggest that PKC may contribute to the physiological regulation of DNA helicase and ATPase activities in the

plant cell. Here we have reported the phosphorylation of eIF4A by PKC. This may also increase our understanding of the link between signal transduction and gene expression in plant systems.

Localization of PDH47 in both cytosol and nucleus indicates that it could be a multifunctional protein. The fact that PDH47 is more abundant in the cytosol than the nucleus makes it different from the previously described PDH45, which was present in almost equal amounts in cytosol and nucleus (Pham *et al.*, 2000). These findings suggest the possibility of a function for PDH47 in initiation of translation (because of its cytosolic localization) and maybe some other role in nucleic acid transaction processes (because of its presence in the nucleus). Previously, the mammalian protein eIF4AIII (isoform of eukaryotic translation initiation factor 4A) has been shown to be present in the nucleus and is involved in nonsense-mediated mRNA decay (Ferraiuolo *et al.*, 2004).

In conclusion, the data in this paper report the cloning and molecular characterization of a unique cold and salinity stress-induced bipolar and dual helicase in pea plants. The discovery of such an important DNA helicase with a possible role in abiotic stress signaling should make a significant contribution to our better understanding of DNA transactions in stressed conditions which have hitherto not been studied in detail in plants.

## Experimental procedures

### Materials

M13 ssDNA and dsDNA were prepared using standard methods. NTPs and dNTPs were from Life Technologies (Gaithersburg, MD, USA), and [ $\gamma$ - $^{32}$ P]-ATP, [ $\alpha$ - $^{32}$ P]-dCTP and [ $S^{35}$ ]-methionine were purchased from Amersham Bioscience (Piscataway, NJ, USA). Synthetic RNA and DNA oligonucleotides were synthesized chemically and purified electrophoretically. The TNT Coupled Wheat Germ Extract System was purchased from Promega. Protein A Sepharose was from Amersham Pharmacia Biotech (Uppsala, Sweden). The helicase enzyme (PDH47) was purified to homogeneity using a bacterial system as a recombinant His-tag protein.

### Plant growth and treatment

Pea (*Pisum sativum*) seeds were surface-sterilized and allowed to grow on wet germination paper under a 14 h/10 h light/dark cycle at room temperature (20–22°C) for 7 days. For salt treatment, the seedlings were grown in 300 mM NaCl solution by dipping the roots only. For temperature treatments, the seedlings were transferred to a 4°C cold chamber or a 37°C chamber under white light. For drought treatment, the seedlings were carefully removed and dehydrated on the filter paper as described by Yamaguchi-Shinozaki and Shinozaki (1994). For ABA treatment 100  $\mu$ M ABA was sprayed on the seedling leaves and also the seedlings were transferred to the same solution by dipping the roots. Seedlings grown in water for the same period of time were taken as a control. After all the treatments, the seedlings were frozen in liquid nitrogen and processed for RNA isolation to analyze the expression of PDH47 transcripts.

### Construction of a *Pisum sativum* cDNA library

A cDNA library was constructed from 5 µg of poly(A)<sup>+</sup> RNA (isolated from the top four leaves of 7-day-grown pea seedlings) in Uni-Zap XR vector using a Zap-cDNA synthesis kit (Stratagene, La Jolla, CA, USA) following the manufacturer's protocol. The resulting phage library contained 10<sup>9</sup> plaque forming units ml<sup>-1</sup>. During library construction, some ds-cDNA was also synthesized from cold-stressed pea seedlings for use as a template for PCR cloning of partial cDNA of stress-induced DNA helicase.

### Stress-induced cDNA clones of pea DNA helicase and their sequence analysis

The stress-induced cDNAs encoding DNA helicase were first partially cloned by PCR and then followed by isolation of full-length clones by library screening. For partial cloning degenerate primers 1 (forward) and 2 (reverse) were designed, which correspond to conserved helicase motif I (AQS<sub>1</sub>GTGK) and motif VI (HRIG<sub>1</sub>RSG), respectively. The sequences of the primers were as follows: primer 1, 5'-GCTCAA<sup>ACT</sup>GGAAC(C/G/T)GG(A/G/T)AA-3'; primer 2, 5'-CCA(C/G/T)(A/G/T)GGACCAATACGATG-3'. In PCR reactions, using respective primer pairs and cold-stressed ds-cDNAs as a template, a partial fragment of 800 bp was amplified. For cloning the full-length cDNAs this partial fragment was radiolabeled and used as probe to screen the pea cDNA library.

The cDNA sequencing was performed using the dideoxy chain termination method with a Sequenase version 2 kit (US Biochemicals, Cleveland, OH, USA). Most of the routine sequence (DNA and amino acid) analysis was performed using MacVector (version 7; Oxford Molecular Group). A homology search was performed using FASTA and multiple sequence alignment was done using CLUSTAL W alignment programs.

### Northern and Western blots

For Northern analysis, total RNA was extracted with TRIzol (Gibco-BRL, Gaithersburg, MD, USA) from different tissues of 7-day-old pea seedlings grown in water. The total RNAs were also extracted from the seedlings exposed to different abiotic stresses (cold, salinity, heat, drought and ABA). About 30 µg of total RNA was resolved by electrophoresis in a 1% agarose gel containing 5.5% formaldehyde, and trans-blotted onto Hybond N<sup>+</sup> membrane with 10× SSC as a transfer buffer. For Southern analysis the genomic DNA (30 µg) was extracted from pea leaves by the standard cetyltrimethylammonium bromide (CTAB) method and digested with an excess of restriction enzymes, electrophoresed on 0.75% agarose gel, and transferred onto a nylon membrane (Hybond N<sup>+</sup>).

The RNA blot was hybridized with [ $\alpha$ -<sup>32</sup>P]-labeled (nick translated) *PDH47* cDNA (full-length) as a probe at 58°C in 5× SSC, 5× Denhardt's, 0.1% SDS and 100 µg ml<sup>-1</sup> denatured salmon sperm DNA for 16–18 h. After hybridization the blots were washed twice for 15 min at low stringency (2× SSC + 0.1% SDS at 50°C) and twice for 15 min at high stringency (0.1× SSC + 0.1% SDS at 55°C) followed by autoradiography. The transcript levels were estimated by scanning the autoradiograph using a laser densitometer (FLUOR-S MULTI IMAGER QUANTITY 1[4.1.1] software; Bio-Rad, Hercules, CA, USA).

For Western analysis, total proteins were extracted from leaves of pea seedlings, fractionated on a 10% polyacrylamide gel followed by electrotransfer onto a nitrocellulose membrane. Anti-PDH47 polyclonal antibodies (rabbit) or anti-His monoclonal antibody followed by alkaline-phosphatase conjugated secondary antibody were used for detection of the PDH47 polypeptide. The signal was

developed by nitroblue tetrazolium (NBT)/5-bromo-4-chloro-3-indolyl phosphate (BCIP) using the standard procedure.

### Construction of plasmid for expression of stress-induced PDH47 protein

The complete coding region (ORF) of the *PDH47* cDNA (1239 bp) was amplified by PCR using ds-cDNA as a template with primers (5' and 3' ORF primers) harboring restriction sites, cloned in frame into the *Bam*HI site of the pET28a vector(+) (Novagen, Madison, WI, USA). The primers were as follows: primer 3, 5'-CGGGATCCATGGCAGGAGTTGCAC-3' (forward) contains *Bam*HI site (underlined); primer 4, 5'-CGGGATCCCTCACAG-AAGTTCAGCC-ACATTG-3' (reverse) contains *Bam*HI site (underlined). This resulted in the construction of plasmid pET28a-*PDH47* whose sequence and orientation were verified before being used for protein expression.

### Expression and purification of PDH47 protein

The plasmid pET28a-*PDH47* was transformed into *E. coli* BL21(DE3) plysS cells (Novagen, Schwalbach, Germany). A fresh culture of the *E. coli* containing pET28a-*PDH47* was grown in Luria-Bertani (LB) medium containing 50 µg ml<sup>-1</sup> of kanamycin (until the Absorbance at 600 nm wavelength [*A*<sub>600</sub>] reached 0.5), induced by IPTG (0.1 mM) and harvested by centrifugation. All the purification steps were performed at 4°C. The resulting pellet was resuspended in ice-cold Tris-buffered saline (TBS) buffer, and lysed by the freeze-thaw method according to Novagen's instructions. The cell lysate was centrifuged at 10 000 *g* for 10 min at 4°C. PDH47 was present in the soluble fraction so it was purified using nickel-NTA (Qiagen GmbH, Cologne, Germany) column chromatography following the manufacturer's instructions. The resulting protein was almost 95% pure as checked by Western blotting. PDH47 was further purified to homogeneity by heparin Sepharose 6B (Pharmacia) column chromatography in buffer containing 50 mM Tris-HCl, pH 7.4, 50 mM KCl, 1 mM EDTA and protease inhibitors. The dialyzed protein was applied to the column and eluted at 250 mM KCl in the same buffer. The purity of the recombinant protein (histidine-tagged PDH47) was checked by SDS-PAGE and Western blotting with anti-PDH47 and anti-His antibodies using standard procedures and this pure protein was used for all assays.

### Preparation of substrate for DNA and RNA helicase assays

The substrate used in the DNA-unwinding assay consisted of a <sup>32</sup>P-labeled 47-mer DNA oligo [5'-(T)<sub>15</sub>GTTTTCCCAGTCACGAC(T)<sub>15</sub>-3'] annealed to M13mp19 phage ssDNA. This partial duplex DNA substrate contained hanging tails of 15 nucleotides at both the 5' and 3' ends. It was prepared as follows: 10 ng of 47-mer was radiolabeled at the 5' end with T4 polynucleotide kinase (5 U) and 0.925 MBq of [ $\gamma$ -<sup>32</sup>P]-ATP (185 TBq mmol<sup>-1</sup>), annealed with 3 µg of M13 ssDNA followed by purification using gel filtration chromatography as described (Tuteja *et al.*, 1994, 1996). DNA-RNA substrates and partial duplex RNA substrates used in this study were described previously (Tuteja *et al.*, 1991, 1992, 1993, 1994, 1996).

### DNA helicase and ATPase assays

The DNA helicase reaction was performed in 10 µl of mixture consisting of 20 mM Tris-HCl (pH 8.0), 2 mM ATP, 0.5 mM MgCl<sub>2</sub>, 75 mM KCl or NaCl, 8 mM DTT, 4% (w/v) sucrose, 80 µg ml<sup>-1</sup> BSA, about 1 ng of <sup>32</sup>P-labeled substrate (approximately 2000 c.p.m.; 40 pm or

0.40 fmol/10  $\mu$ l) and the purified PDH47 protein (10 ng; 20 nM or 0.20 pmol/10  $\mu$ l). The reaction mixture was incubated for 60 min at 37°C and the reaction was stopped and analyzed as previously described (Tuteja *et al.*, 1994). The ATPase reaction conditions were identical, except that the  $^{32}$ P-labeled helicase substrate and 2 mM ATP were omitted and instead 1665 Bq [ $\gamma$ - $^{32}$ P]-ATP was included. This reaction was run for 2 h at 37°C and analyzed as described (Tuteja *et al.*, 1994, 1996).

#### UV cross-linking of ATP to PDH47

Affinity labeling of purified PDH47 protein with [ $\alpha$ - $^{32}$ P]-ATP was performed as previously described (Tuteja *et al.*, 1993). *Escherichia coli* DNA polymerase I was used as a positive control.

#### Immunodepletion of helicase and ATPase activities of PDH47

The immunodepletion of enzymatic activities of PDH47 was performed as described previously (Tuteja *et al.*, 2001). Polyclonal antibodies against recombinant PDH47 were raised in rabbits. The IgG from immune and pre-immune sera was purified using protein A-Sepharose by standard procedures. Since the recombinant PDH47 was purified as a His-tag protein, monoclonal anti-His antibody was also used for immunodepletion. PDH47 protein was first incubated with anti-PDH47 IgG or monoclonal antibody followed by removal of antigen-antibody complex by protein A Sepharose beads. Measurement of enzymatic activities in the supernatant was as described.

#### ATP-dependent RNA helicase and DNA-RNA helicase assays

The RNA-RNA- and DNA-RNA-unwinding reaction conditions were identical to those described above for the DNA helicase reaction, except the DNA substrate was replaced by  $^{32}$ P-labeled RNA-RNA or DNA-RNA partial duplex substrates and one unit of RNase block was also included in the reaction.

#### In vitro translation

For *in vitro* transcription and translation of the luciferase gene, TNT Coupled Wheat Germ Lysate from Promega along with [ $^{35}$ S]-methionine was used as described by the manufacturer. Before the reaction the wheat germ lysate was incubated for 10 min at 4°C with either pre-immune IgG or anti-PDH47 IgG. The IgG from rabbit sera was purified by protein A Sepharose using standard procedures. The standard reaction (without any antibodies) was also performed in the presence of purified PDH47 protein.

#### Protein kinase assay

*In vitro* phosphorylation of PDH47 was performed with PKC from an animal source (Promega). For the PKC assay, 50  $\mu$ l of the reaction mixture contained 30 mM HEPES, (pH 7.5), 10 mM MgCl<sub>2</sub>, 2 mM CaCl<sub>2</sub>, 5 mM EGTA, 4  $\mu$ g of phosphatidylserine (PS), 10 nM phorbol 12-myristate 13-acetate (PMA), 40 ng (or 60 ng) of purified PDH47 protein and 5 U PKC. The reaction was initiated by adding [ $\gamma$ - $^{32}$ P]-ATP to a final concentration of 1  $\mu$ M (2  $\mu$ Ci) and incubated at 30°C for 30 min. The addition of 13  $\mu$ l of 4 $\times$  Laemmli SDS sample buffer terminated the reaction. This was loaded on a SDS-10% polyacrylamide gel, fractionated by electrophoresis and analyzed by autoradiography.

#### Phospho-amino acid analysis

The phosphorylated 47 kDa band of PDH47 was eluted from the gel and hydrolyzed in 6 N HCl for 2 h at 100°C as described (Hunter and Sefton, 1980). After hydrolysis, the sample was concentrated in a Speed Vac and analyzed by paper chromatography on Whatman 3 MM paper. The standard samples (phosphoserine, phosphotyrosine and phosphothreonine) were also run along with this sample. After chromatography the paper was sprayed with ninhydrin followed by autoradiography.

#### Preparation of pea nuclear extract, cytosol and chloroplast lysate

Pea nuclear extract and cytosol were prepared from 7–8-day-old pea seedlings as previously described (Tuteja *et al.*, 2001). The chloroplast lysate was prepared as described (Tuteja *et al.*, 1996).

#### In vivo localization by immunofluorescence staining and confocal microscopy

Exponentially growing tobacco BY2 suspension cells were fixed in 4% formaldehyde, permeabilized by cellulase and layered onto poly-L-lysine-coated cover slips. The cells were immunostained with PDH47-specific primary rabbit antibody in 1:2000 dilutions and Alexafluor 488-labeled goat antirabbit secondary antibody (Molecular Probes, Eugene, OR, USA) in 1:1000 dilutions. The cells were counter-stained with 4',6-diamidino-2-phenylindole (DAPI) (0.2  $\mu$ g ml<sup>-1</sup>) for 20 min just before mounting the slide in Antifade solution (Fluoroguard; Bio-Rad, USA). Confocal laser scanning (Radiance 2100; Bio-Rad) was performed under a Nikon microscope (objective Plane Apo 60 $\times$ /1.4 oil; Nikon Corporation, Tokyo, Japan). The excitation wavelength for Alexa fluorescence was 488 nm (argon laser) and fluorescence was detected through an HQ515/30 emission filter (high-quality band pass), centered at 515 nm with 30 nm bandwidth. DAPI fluorescence was excited by a blue diode (405 nm) and detected through an HQ442/45 emission filter. Image processing was carried out with LazerSharp (Bio-Rad) and PhotoShop 5.5 (Adobe systems, San Jose, CA, USA) was used for the final image assembly.

#### Acknowledgements

We are grateful to Dr Robert Haselkorn (University of Chicago, USA) and Dr Kanury Rao (ICGEB, New Delhi) for correcting the manuscript and Dr Badri Nath Singh (ICGEB, New Delhi) for his help in the localization study. The confocal microscope facility at ICGEB, New Delhi, is funded by an International Senior Research Fellowship of the Wellcome Trust (UK). This work was partially supported by grants from the Department of Biotechnology, Government of India and Defence Research and Development Organization, Government of India. We also thank the Council of Scientific and Industrial Research, New Delhi for a fellowship to A.A.V.

#### References

- Anand, S.P. and Khan, S.A. (2004) Structure-specific DNA binding and bipolar helicase activities of PcrA. *Nucleic Acids Res.* **32**, 3190–3197.

- Briolat, V. and Reysset, G.** (2002) Identification of the *Clostridium perfringens* genes involved in the adaptive response to oxidative stress. *J. Bacteriol.* **184**, 2333–2343.
- Buelt, M.K., Glidden, B.J. and Storm, D.R.** (1994) Regulation of p68 RNA helicase by calmodulin and protein kinase C. *J. Biol. Chem.* **269**, 29 367–29 370.
- op den Camp, R.G. and Kuhlemeier, C.** (1998) Phosphorylation of tobacco eukaryotic translation initiation factor 4A upon pollen tube germination. *Nucleic Acids Res.* **26**, 2058–2062.
- Chamot, D., Magee, W.C., Yu, E. and Owtrim, G.W.** (1999) A cold shock-induced cyanobacterial RNA helicase. *J. Bacteriol.* **181**, 1728–1732.
- Charollais, J., Dreyfus, M. and Iost, I.** (2004) CsdA, a cold-shock RNA helicase from *Escherichia coli*, is involved in the biogenesis of 50S ribosomal subunit. *Nucleic Acids Res.* **32**, 2751–2759.
- Constantinesco, F., Forterre, P., Koonin, E.V., Aravind, L. and Elie, C.A.** (2004) Bipolar DNA helicase gene, herA, clusters with rad50, mre11 and nurA genes in thermophilic archaea. *Nucleic Acids Res.* **32**, 1439–1447.
- Ferraiuolo, M.A., Lee, C.S., Ler, L.W., Hsu, J.L., Costa-Mattioli, M., Luo, M.J., Reed, R. and Sonenberg, N.** (2004) A nuclear translation-like factor eIF4AIII is recruited to the mRNA during splicing and functions in nonsense-mediated decay. *Proc. Natl Acad. Sci. USA*, **101**, 4118–4123.
- Gingras, A.C., Raught, B. and Sonenberg, N.** (1999) eIF4 Initiation factors: effectors of mRNA recruitment to ribosomes and regulators of translation. *Annu. Rev. Biochem.* **68**, 913–963.
- Gong, Z., Lee, H., Xiong, L., Jagendorf, A., Stevenson, B. and Zhu, J.-K.** (2002) RNA helicase-like protein as an early regulator of transcription factors for plant chilling and freezing tolerance. *Proc. Natl Acad. Sci. USA*, **99**, 11507–11512.
- Gorbalenya, A.E., Koonin, E.V., Donchenko, A.P. and Blinov, V.M.** (1989) Two related superfamilies of putative helicases involved in replication, recombination, repair and expression DNA and RNA genomes. *Nucleic Acids Res.* **17**, 4713–4730.
- Hunter, T. and Sefton, B.M.** (1980) Transforming gene product of Rous sarcoma virus phosphorylates tyrosine. *Proc. Natl Acad. Sci. USA*, **77**, 1311–1315.
- Linder, P., Lasko, P.F., Ashburner, M., Leroy, P., Nielsen, P.J., Nishi, K., Schnier, J. and Slonimski, P.P.** (1989) Birth of the D-E-A-D box. *Nature*, **337**, 121–122.
- Liu, H.Y., Nefsky, B.S. and Walworth, N.C.** (2002) The Ded1 DEAD-box helicase interacts with Chk1 and Cdc2. *J. Biol. Chem.* **277**, 2637–2643.
- Lohman, T.M. and Bjornson, K.P.** (1996) Mechanism of helicase-catalyzed DNA unwinding. *Annu. Rev. Biochem.* **65**, 169–214.
- Luking, A., Stahl, U. and Schmidt, U.** (1998) Protein family of RNA helicases. *Crit. Rev. Biochem. Mol. Biol.* **33**, 259–296.
- Matson, S.W., Bean, D. and George, J.W.** (1994) DNA helicases; enzymes with essential roles in all aspects of DNA metabolism. *Bioessays*, **16**, 13–21.
- Nakamura, T., Muramoto, Y. and Takabe, T.** (2004) Structural and transcriptional characterization of a salt-responsive gene encoding putative ATP-dependent RNA helicase in barley. *Plant Sci.* **167**, 63–70.
- Pause, A. and Sonenberg, N.** (1992) Mutational analysis of a DEAD-box RNA helicase; the mammalian translation initiation factor eIF-4A. *EMBO J.* **11**, 2643–2654.
- Pham, X.H., Reddy, M.K., Ehtesham, N.Z., Matta, B. and Tuteja, N.** (2000) A DNA helicase from *Pisum sativum* is homologous to translation initiation factor and stimulates topoisomerase activity. *Plant J.* **24**, 219–229.
- Sanan-Mishra, N., Pham, X.H., Sopory, S.K. and Tuteja, N.** (2005) Pea DNA helicase 45 overexpression in tobacco confers high salinity tolerance without affecting yield. *Proc. Natl Acad. Sci. USA*, **102**, 509–514.
- Seki, M., Narusaka, M., Abe, H., Kasuga, M., Yamaguchi-Shinozaki, K., Carninci, P., Hayashizaki, Y. and Shinozaki, K.** (2001) Monitoring the expression pattern of 1300 Arabidopsis genes under drought and cold stresses by using a full-length cDNA microarray. *Plant Cell*, **13**, 61–72.
- Tuteja, N.** (2003) Plant DNA helicases: the long unwinding road. *J. Exp. Bot.* **54**, 2201–2214.
- Tuteja, N. and Tuteja, R.** (1996) DNA helicases: the long unwinding road. *Nat. Genet.* **13**, 11–12.
- Tuteja, N. and Tuteja, R.** (2004a) Prokaryotic and eukaryotic DNA helicases. Essential molecular motor proteins for cellular machinery. *Eur. J. Biochem.* **271**, 1835–1848.
- Tuteja, N. and Tuteja, R.** (2004b) Unraveling DNA helicases. Motif, structure, mechanism and function. *Eur. J. Biochem.* **271**, 1849–1863.
- Tuteja, N., Rahman, K., Tuteja, R. and Falaschi, A.** (1991) DNA helicase IV from HeLa cells. *Nucleic Acids Res.* **19**, 3613–3618.
- Tuteja, N., Rahman, K., Tuteja, R., Ochem, A., Skopac, D. and Falaschi, A.** (1992) DNA helicase III from HeLa cells: an enzyme that acts preferentially on partially unwound DNA duplexes. *Nucleic Acids Res.* **20**, 5329–5337.
- Tuteja, N., Rahman, K., Tuteja, R. and Falaschi, A.** (1993) Human DNA helicase V, a novel DNA unwinding enzyme from HeLa cells. *Nucleic Acids Res.* **21**, 2323–2329.
- Tuteja, N., Tuteja, R., Ochem, A. et al.** (1994) Human DNA helicase II: a novel DNA unwinding enzyme identified as the Ku autoantigen. *EMBO J.* **13**, 4991–5001.
- Tuteja, N., Phan, T.-N. and Tewari, K.K.** (1996) Purification and characterization of a DNA helicase from pea chloroplast that translocates in the 3' to 5' direction. *Eur. J. Biochem.* **238**, 54–63.
- Tuteja, N., Beven, A.F., Shaw, P.J. and Tuteja, R.** (2001) A pea homologue of human DNA helicase I is localized within the dense fibrillar component of the nucleolus and stimulated by phosphorylation with CK2 and cdc2 protein kinases. *Plant J.* **25**, 9–17.
- Tuteja, N., Reddy, M.K., Mudgil, Y., Yadav, B.S., Chandok, M. and Sopory, S.K.** (2003) Pea DNA topoisomerase I is phosphorylated and stimulated by casein kinase 2 and protein kinase C. *Plant Physiol.* **132**, 2108–2115.
- Yamaguchi-Shinozaki, K. and Shinozaki, K.** (1994) A novel cis-acting element in an *Arabidopsis* gene is involved in responsiveness to drought, low-temperature, or high-salt stress. *Plant Cell*, **6**, 251–264.
- Yang, L., Yang, J., Youliang, H. and Liu, Z.-R.** (2004) Phosphorylation of p68 RNA helicase regulates RNA binding by the C-terminal domain of the protein. *Biochem. Biophys. Res. Commun.* **314**, 622–630.
- Yu, E. and Owtrim, G.W.** (2000) Characterization of the cold stress-induced cyanobacterial DEAD-box protein CrhC as an RNA helicase. *Nucleic Acids Res.* **28**, 3926–3934.

Data deposition: The sequences reported in this paper have been deposited in the GenBank database (accession no. AY167670).